nature physics

LETTERS

https://doi.org/10.1038/s41567-019-0670-x

Extreme magnetic field-boosted superconductivity

Sheng Ran[1,2,3*], I-Lin Liu[1,2,3], Yun Suk Eo[1], Daniel J. Campbell[1], Paul M. Neves[1], Wesley T. Fuhrman[1], Shanta R. Saha[1,2], Christopher Eckberg[1], Hyunsoo Kim[1], David Graf[4], Fedor Balakirev[5], John Singleton[5,6], Johnpierre Paglione[1,2] and Nicholas P. Butch[1,2*]

Applied magnetic fields underlie exotic quantum states, such as the fractional quantum Hall effect[1] and Bose–Einstein condensation of spin excitations[2]. Superconductivity, however, is inherently antagonistic towards magnetic fields. Only in rare cases[3–5] can these effects be mitigated over limited fields, leading to re-entrant superconductivity. Here, we report the coexistence of multiple high-field re-entrant superconducting phases in the spin-triplet superconductor UTe_2 (ref. [6]). We observe superconductivity in the highest magnetic field range identified for any re-entrant superconductor, beyond 65 T. Although the stability of superconductivity in these high magnetic fields challenges current theoretical models, these extreme properties seem to reflect a new kind of exotic superconductivity rooted in magnetic fluctuations[7] and boosted by a quantum dimensional crossover[8].

It is a basic fact that magnetic fields are destructive to superconductivity. The maximum magnetic field in which superconductivity survives, the upper critical field H_{c2}, is restricted by both the paramagnetic effect of electron spin polarization due to the Zeeman effect and the orbital pair-breaking effect of electron–cyclotron motion due to the Lorentz force. In a few very rare cases, however, magnetic fields can do the opposite and actually stabilize superconductivity[3–5]. In these cases, the applied magnetic field is most often compensated by an internal field produced by ordered magnetic moments through exchange interactions, resulting in a reduced total effective field[9]. A different set of circumstances involving unconventional superconductivity occurs in the ferromagnetic superconductor URhGe (refs. [10,11]), in which field-induced superconductivity is attributed to very strong ferromagnetic fluctuations that emanate from a quantum instability of a ferromagnetic phase, strengthening spin-triplet pairing[7].

Here, we report the presence of two independent high-field superconducting phases in the recently discovered triplet superconductor UTe_2 (ref. [6]), for a total of three superconducting phases (Fig. 1). This is an example of two field-induced superconducting phases existing in one system, one of which has the highest lower and upper limiting fields of any field-induced superconducting phase: more than 40 T and 65 T, respectively. It is probable that both of the field-induced superconducting phases are stabilized by ferromagnetic fluctuations that are induced when the magnetic field is applied perpendicular to the preferred direction of the electron spins. The high-field superconducting phase exists exclusively in a magnetic field-polarized state, unique among these superconductors. This discovery provides an excellent platform to study the relationship between ferromagnetic fluctuations, spin-triplet superconducting pairing and dimensionality in the quantum limit.

UTe_2 crystallizes in an anisotropic orthorhombic structure, with the a axis the magnetic easy axis along which spins prefer to align in low magnetic fields. H_{c2} is strongly direction-dependent and exceedingly large along the b axis, with an unusual increase in its temperature dependence above 15 T. H_{c2} is extraordinarily sensitive to the alignment of the magnetic field along the b axis[12], and accurate measurements require the use of a specialized two-axis rotator (Fig. 1b). When the magnetic field is perfectly aligned along the b axis, superconductivity persists up to 34.5 T at 0.35 K (Fig. 2a). A small misalignment of less than 5° from the b axis towards the a axis decreases the H_{c2} value by over half, to 15.8 T. However, even this misaligned superconductivity is resilient: when the magnetic field is further increased, superconductivity reappears between 21 T and 30 T. Our measurements show that this re-entrant phase, SC_{RE}, does not persist beyond misalignment greater than 7°. When the field is rotated towards the c axis, SC_{RE} does not persist beyond 3.9° (Supplementary Fig. 1). Future measurements will determine whether this phase boundary exhibits similar curvature.

Although UTe_2 is closely related to the ferromagnetic triplet superconductors[6], the observation of re-entrant superconductivity in UTe_2 resembles neither that of URhGe (refs. [10,11]), which is completely separated from the low-field portion, nor the sharp H_{c2} cusp in angle dependence[13] in UCoGe. The angle dependence of the superconducting phase boundary suggests that SC_{RE} may have a distinct order parameter from the lower-field superconductivity, SC_{PM}. However, unlike the case for both URhGe (refs. [11,14]) and UCoGe (refs. [13,15]), there is no normal-state change in the underlying magnetic order in UTe_2 that would drive a change in the superconducting order parameter symmetry. We discuss the magnetic interactions that stabilize this unusual behaviour after an excursion to an even higher field.

The upper-field limit of SC_{RE} of 35 T coincides with a dramatic magnetic transition into a field-polarized phase (Fig. 2c). The magnetic moment along the b axis jumps from 0.35 to 0.65 μ_B discontinuously, due to a spin rotation from the easy a axis to the orthogonal b axis. The abrupt change in moment direction is accompanied by a jump in magnetoresistance R and a sudden change of frequency f in the proximity detector oscillator (PDO) circuit (Fig. 2b). The critical field H_m of this magnetic transition has little temperature dependence up to 10 K, but H_m increases as the magnetic field rotates away from the b axis to either the a or c axis (Fig. 1c). Meanwhile, the magnitude of the jump in magnetic moment, 0.3 μ_B, seems to

[1]Center for Nanophysics and Advanced Materials, Department of Physics, University of Maryland, College Park, MD, USA. [2]NIST Center for Neutron Research, National Institute of Standards and Technology, Gaithersburg, MD, USA. [3]Department of Materials Science and Engineering, University of Maryland, College Park, MD, USA. [4]National High Magnetic Field Laboratory, Florida State University, Tallahassee, FL, USA. [5]National High Magnetic Field Laboratory, Los Alamos National Laboratory, Los Alamos, NM, USA. [6]Department of Physics, The Clarendon Laboratory, University of Oxford, Oxford, UK. *e-mail: sran@umd.edu; nbutch@umd.edu

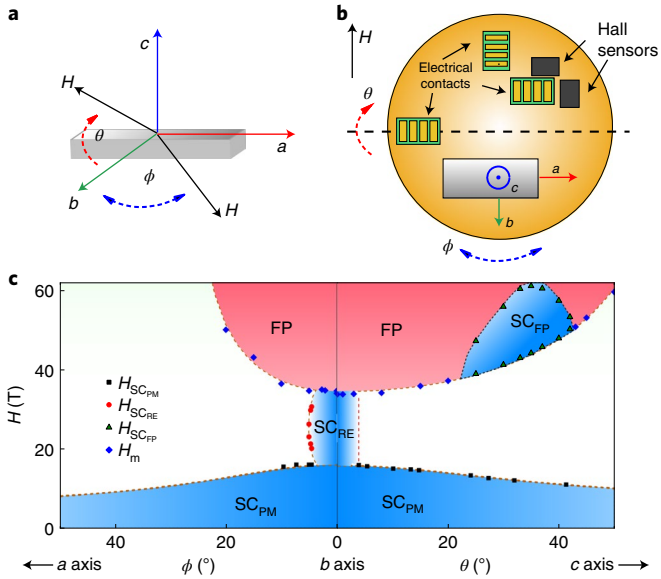

Fig. 1 | Magnetic field-induced superconducting and polarized phases of UTe_2. a, Sketch of how the magnetic field is applied with respect to the three crystallographic axes of UTe_2. **b**, Top view of the sample platform with a two-axis rotator used in d.c. field measurements to achieve the best alignment. **c**, Magnetic field–angle phase diagram showing the three superconducting phases SC_{PM}, SC_{RE} and SC_{FP}. FP is the field-polarized phase. The magnetic field is rotated within the *a*–*b* and *b*–*c* planes. The critical field values of the SC_{PM} and SC_{RE} phases are based on d.c. field measurements, and those of the SC_{FP} and FP phases are based on pulsed field measurements. The SC_{RE} phase was not observed for angles of θ larger than 3.9° in the *b*–*c* plane (Supplementary Fig. 1). The dashed lines are guides to the eye.

be direction-independent (Supplementary Fig. 5). This magnetic field scale seems to represent a general energy scale for correlated uranium compounds: weak anomalies are observed in the ferromagnetic superconductor UCoGe (ref. [16]), whereas a large magnetization jump occurs in the hidden-order compound URu_2Si_2 (ref. [17]).

As H_m limits the SC_{RE} phase, it gives rise to an even more startling form of superconductivity. Sweeping magnetic fields through the angular range of $\theta = 20$–$40°$ from the *b* axis towards the *c* axis reveals a superconducting phase inside the field-polarized state SC_{FP} at high *H* (Fig. 3). The onset field of the SC_{FP} phase precisely follows the angle dependence of H_m, while the upper critical field goes through a dome, with the maximum value exceeding 65 T, the maximum field possible in our measurements. This new superconducting phase largely exceeds the magnetic field range of all known field-induced superconductors[3–5,10]. Owing to its shared phase boundary with the magnetic transition, this superconducting phase tolerates a rather large angular range of offsets from the *b*–*c* rotation plane. However, it does not appear when the field is rotated from the *b* axis to the *a* axis.

Having established the field limits and angle dependence of the SC_{FP} phase, we turn to its temperature stability (Fig. 4). The onset field has almost no temperature dependence, again following H_m, while the upper critical field of the SC_{FP} phase disappears near 1.6 K, similar to the zero-field superconducting critical temperature. This suggests that although it is stabilized at a remarkably high field, the new superconducting phase involves a similar pairing energy scale to the zero-field superconductor.

The mechanism responsible for the large magnetic field and temperature stability of the SC_{FP} phase is unclear. A natural candidate is the Jaccarino–Peter effect used to describe other re-entrant superconductors[9]. This antiferromagnetic type of exchange interaction can lead to an internal magnetic field that is opposite the external magnetic field, resulting in a much smaller total magnetic field. This compensation mechanism has successfully explained the field-induced superconductivity in Chevrel-phase compounds and organic superconductors[3–5], but it probably does not apply to the SC_{FP} phase of UTe_2, which lacks the requisite localized atomic moments. Furthermore, SC_{FP} persists over a wider field–angle range than is typical of the compensation effect[18].

The temperature dependence of the SC_{FP} phase and its close relationship with the magnetic transition are reminiscent of the field-induced superconducting phase in URhGe, which has been attributed to ferromagnetic spin fluctuations associated with the competition of spin alignment between two weakly anisotropic axes. In URhGe, a magnetic field transverse to the direction of the ordered magnetic moments leads to the collapse of the Ising ferromagnetism; this instability enhances ferromagnetic fluctuations, which in turn induce superconductivity[7].

UTe_2, however, is not ferromagnetic. Nevertheless, the similarities between UTe_2 and the ferromagnetic superconductors with regard to the relationship between the preferred magnetic axis and the direction of high H_{c2} (ref. [6]) suggest that strong spin fluctuations transverse to the preferred orientation or easy axis of the magnetic moment play a central role in these superconducting phases[7]. The H_{c2} values and directionality in UTe_2 can thus be understood in the following manner. Starting from zero magnetic field, superconductivity is most resilient to a magnetic field applied along the *b* axis, which is perpendicular to the easy magnetic *a* axis. A magnetic field applied along the *b* axis thus induces spin fluctuations that stabilize superconductivity against field-induced pair breaking. At 34.5 T, however, a magnetic phase transition occurs, and magnetic moments rotate from the *a* axis to the *b* axis. In the high-field-polarized phase, a magnetic field along the *b* axis no longer induces transverse spin fluctuations, and superconductivity is suppressed completely. However, it is possible to induce transverse spin fluctuations by applying a magnetic field along the *c* axis. When viewed as a vector sum of fields along the *b* and *c* axes (Fig. 3), it is clear that H_b stabilizes the magnetic phase, while a range of H_c strength values stabilize superconductivity with the highest re-entrant magnetic field values observed.

This ferromagnetic fluctuation scenario is qualitatively consistent with the wider picture of field-induced superconducting phases in UTe_2, yet a very important distinction exists between the SC_{FP} phase and the field-induced superconducting phase in URhGe: the SC_{FP} phase exists only in the field-polarized state. This challenges the current theory proposed for URhGe, which allows superconductivity to exist on both sides of the phase boundary[7,19,20].

Through the suppression of the orbital limit, reduced dimensionality has been theorized to stabilize high-field superconductivity[21]. A model proposed by Lebed and Sepper[8] invoking spin-triplet pairing predicts re-entrant superconductivity at very high magnetic fields applied transverse to the axis of a quasi-one-dimensional conductor. The field-induced lower dimensionality is field–angle dependent and facilitates the recovery of the zero-field superconducting critical temperature, as we observe in SC_{FP} (Figs. 3 and 4). The possibility that field-stabilizing effects may also exist in quasi-two-dimensional superconductors[21] suggests that high-field dimensionality is a useful starting point for understanding the SC_{FP} phase. Furthermore, the suppression of the orbital limit permits superconductivity in a pure material to survive in any magnetic field, making UTe_2 an exciting basis for further testing of the limits of high-field-boosted superconductivity.

The existence of the SC_{FP} phase in only the field-polarized state, and in such a high magnetic field, suggests that the superconducting state probably has odd parity with time-reversal symmetry breaking.

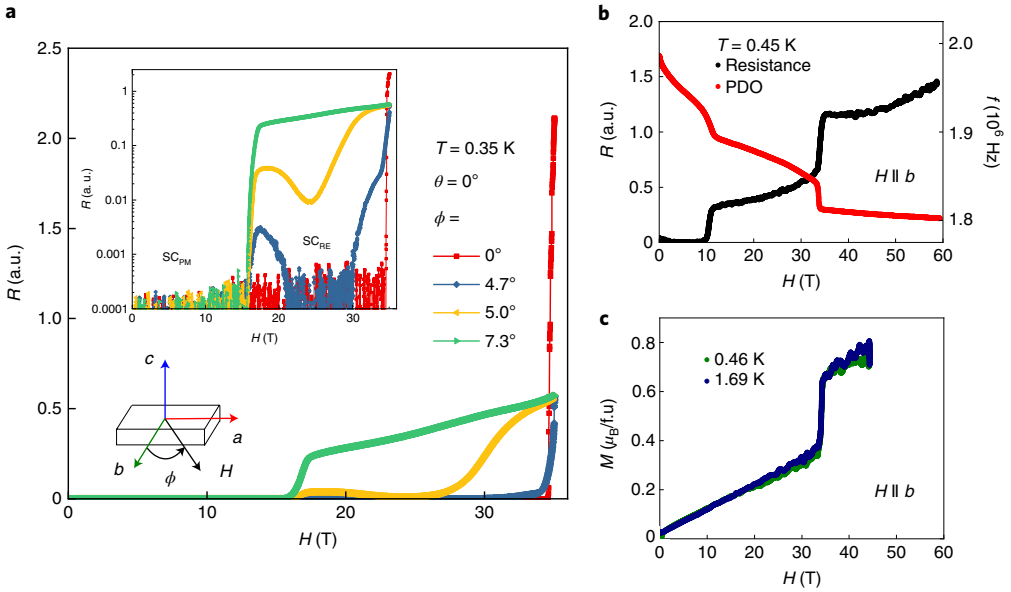

Fig. 2 | Re-entrance of superconductivity in UTe_2. a, Field dependence of R in UTe_2 at $T = 0.35$ K measured in the d.c. field. The magnetic field is rotated from the b axis towards the a axis. Zero resistance persists up to 34.5 T when the magnetic field is perfectly along the b axis. The same dataset is plotted on a logarithmic scale in the inset. Re-entrance of superconductivity can be clearly seen when the magnetic field is applied slightly off the b axis. **b**, Magnetoresistance R and f of the PDO circuit (see Methods for technical details) in UTe_2 at $T = 0.45$ K in the pulsed field, with the magnetic field applied along the b axis. **c**, Magnetization measurements of UTe_2 at $T = 0.46$ K and 1.69 K in the pulsed field, with the magnetic field applied along the b axis. The two-axis rotator is not compatible with measurements in the pulsed field. There is probably a slight angle offset along the perpendicular direction. SC_{RE} is not observed in these measurements. f.u., formula unit.

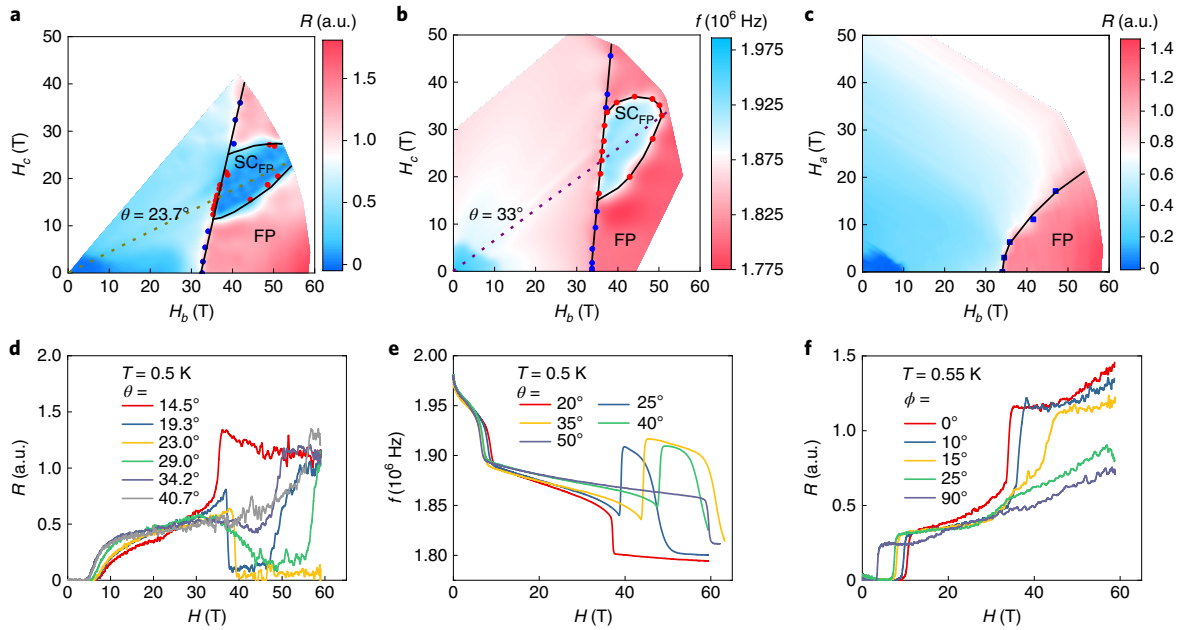

Fig. 3 | Angle dependence of the field-induced superconducting and polarized phases of UTe_2. a–**c**, When the magnetic field is applied at an angle from the b axis towards the c axis (or a axis), it is equivalent to two applied magnetic fields: one along the b axis, $H_b = H\cos\theta$ or $H\cos\phi$, and the other along the c axis, $H_c = H\sin\theta$ (or along the a axis, $H_a = H\sin\phi$). Colour contour plots are shown for magnetoresistance R as a function of H_c and H_b (**a**), f of the PDO circuit as a function of H_c and H_b (**b**), and magnetoresistance R as a function of H_a and H_b (**c**). The blue dots are the critical fields for the field-polarized state and the red dots are the critical fields for SC_{FP}. The dotted lines in **a** and **b** indicate the directions along which measurements were also performed at different temperatures, as shown in Fig. 4. **d**–**f**, The corresponding data as a function of the applied magnetic fields at selected angles.

Odd parity is the cornerstone of topological superconductivity[22], and it is certain that the SC_{FP} phase has non-trivial topology. Since time-reversal symmetry is also broken, a special topological superconducting state is highly likely, such as chiral superconductivity[23], which hosts Majorana zero modes, the building blocks for topological quantum computing[24,25].

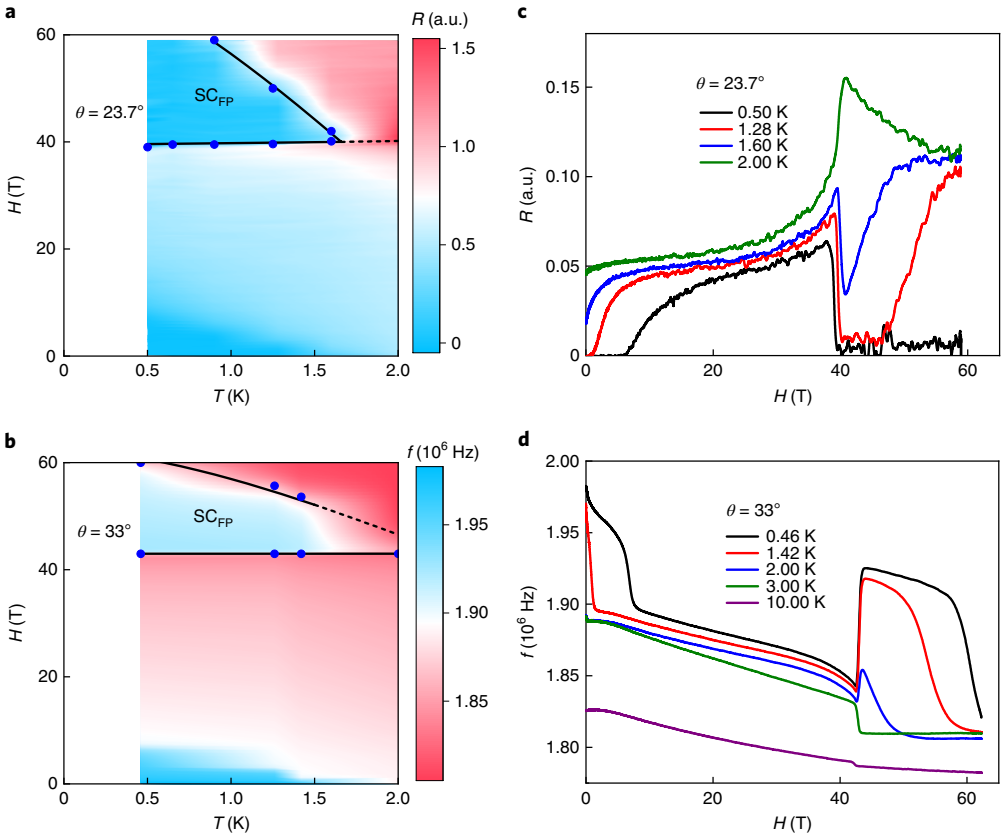

Fig. 4 | Temperature dependence of SC_{FP} in UTe_2. **a**,**b**, Colour contour plots of R (**a**) and f (**b**) of PDO measurements as a function of T and H at $\theta = 23.7°$ (**a**) and $\theta = 33°$ (**b**). The blue dots are the critical fields for SC_{FP} and the dashed lines are guides to the eye, extrapolated to the region where there are no data. **c**,**d**, The corresponding data as a function of the applied magnetic fields at selected temperatures.

Note added in proof: While our manuscript has been under review, we became aware of other independent reports of the field-polarized state[26] and the lower-field re-entrant superconductivity[27] in UTe_2.

Online content

Any methods, additional references, Nature Research reporting summaries, source data, statements of code and data availability and associated accession codes are available at https://doi.org/10.1038/s41567-019-0670-x.

Received: 3 May 2019; Accepted: 21 August 2019;
Published online: 07 October 2019

References

1. Stormer, H. L. Nobel lecture: the fractional quantum Hall effect. *Rev. Mod. Phys.* **71**, 875–889 (1999).
2. Zapf, V., Jaime, M. & Batista, C. D. Bose–Einstein condensation in quantum magnets. *Rev. Mod. Phys.* **86**, 563–614 (2014).
3. Meul, H. W. et al. Observation of magnetic-field-induced superconductivity. *Phys. Rev. Lett.* **53**, 497–500 (1984).
4. Uji, S. et al. Magnetic-field-induced superconductivity in a two-dimensional organic conductor. *Nature* **410**, 908–910 (2001).
5. Konoike, T. et al. Magnetic-field-induced superconductivity in the antiferromagnetic organic superconductor κ–$(BETS)_2FeBr_4$. *Phys. Rev. B* **70**, 094514 (2004).
6. Ran, S. et al. Nearly ferromagnetic spin-triplet superconductivity. *Science* **365**, 684–687 (2019).
7. Mineev, V. P. Reentrant superconductivity in URhGe. *Phys. Rev. B* **91**, 014506 (2015).
8. Lebed, A. G. & Sepper, O. Quantum limit in a magnetic field for triplet superconductivity in a quasi-one-dimensional conductor. *Phys. Rev. B* **90**, 024510 (2014).
9. Jaccarino, V. & Peter, M. Ultra-high-field superconductivity. *Phys. Rev. Lett.* **9**, 290–292 (1962).
10. Lévy, F., Sheikin, I., Grenier, B. & Huxley, A. D. Magnetic field-induced superconductivity in the ferromagnet URhGe. *Science* **309**, 1343–1346 (2005).
11. Lévy, F., Sheikin, I. & Huxley, A. Acute enhancement of the upper critical field for superconductivity approaching a quantum critical point in URhGe. *Nat. Phys.* **3**, 460–463 (2007).
12. Aoki, D. et al. Unconventional superconductivity in heavy fermion UTe_2. *J. Phys. Soc. Jpn* **88**, 043702 (2019).
13. Aoki, D. et al. Extremely large and anisotropic upper critical field and the ferromagnetic instability in UCoGe. *J. Phys. Soc. Jpn* **78**, 113709 (2009).
14. Huxley, A. D., Yates, S. J. C., Lévy, F. & Sheikin, I. Odd-parity superconductivity and the ferromagnetic quantum critical point. *J. Phys. Soc. Jpn* **76**, 051011 (2007).
15. Hattori, T. et al. Relationship between ferromagnetic criticality and the enhancement of superconductivity induced by transverse magnetic fields in UCoGe. *J. Phys. Soc. Jpn* **83**, 073708 (2014).
16. Knafo, W. et al. High-field moment polarization in the ferromagnetic superconductor UCoGe. *Phys. Rev. B* **86**, 184416 (2012).
17. De Boer, F. R. et al. High-magnetic-field and high-pressure effects in monocrystalline URu_2Si_2. *Phys. B+C.* **138**, 1–6 (1986).
18. Balicas, L. et al. Superconductivity in an organic insulator at very high magnetic fields. *Phys. Rev. Lett.* **87**, 067002 (2001).
19. Hattori, K. & Tsunetsugu, H. *p*-Wave superconductivity near a transverse saturation field. *Phys. Rev. B* **87**, 064501 (2013).
20. Sherkunov, Y., Chubukov, A. V. & Betouras, J. J. Effects of Lifshitz transitions in ferromagnetic superconductors: the case of URhGe. *Phys. Rev. Lett.* **121**, 097001 (2018).
21. Dupuis, N. & Montambaux, G. Superconductivity of quasi-one-dimensional conductors in a high magnetic field. *Phys. Rev. B* **49**, 8993–9008 (1994).
22. Sato, M. & Ando, Y. Topological superconductors: a review. *Rep. Prog. Phys.* **80**, 076501 (2017).
23. Kallin, C. & Berlinsky, J. Chiral superconductors. *Rep. Prog. Phys.* **79**, 054502 (2016).
24. Sarma, S. D., Freedman, M. & Nayak, C. Majorana zero modes and topological quantum computation. *npj Quant. Inf.* **1**, 15001 (2015).

25. Karzig, T. et al. Scalable designs for quasiparticle-poisoning-protected topological quantum computation with Majorana zero modes. *Phys. Rev. B* **95**, 235305 (2017).
26. Miyake, A. et al. Metamagnetic transition in heavy fermion superconductor UTe_2. *J. Phys. Soc. Jpn* **88**, 063706 (2019).
27. Knebel, G. et al. Field-reentrant superconductivity close to a metamagnetic transition in the heavy-fermion superconductor UTe_2. *J. Phys. Soc. Jpn* **88**, 063707 (2019).

Acknowledgements

We acknowledge helpful discussions with A. Lebed and V. Yakovenko. W.T.F. is grateful for the support of the Schmidt Science Fellows programme in partnership with the Rhodes Trust. Research at the University of Maryland was supported by the US National Science Foundation Division of Materials Research Award No. DMR-1610349 (support for sample preparation), the US Department of Energy (DOE) Award No. DE-SC-0019154 (support for experimental measurements) and the Gordon and Betty Moore Foundation's EPiQS Initiative through Grant No. GBMF4419 (support for materials synthesis). Work performed at NHMFL was supported by NSF Cooperative Agreement No. DMR-1644779, the State of Florida, DOE and through the DOE Basic Energy Sciences Field Work Project Science in 100 T. A portion of this work was supported by the NHMFL User Collaboration Grants Program. Identification of commercial equipment does not imply recommendation or endorsement by NIST.

Author contributions

N.P.B. directed the project. S.R., W.T.F. and S.R.S. synthesized the single crystalline samples. S.R., I.-L.L., J.S. and F.B. performed the magnetoresistance, PDO and magnetization measurements in the pulsed field. Y.S.E., D.J.C., P.M.N. and D.G. performed the magnetoresistance measurements in the d.c. field. C.E. and H.K. performed magnetoresistance measurements in low magnetic fields. S.R. and N.P.B. wrote the manuscript with contributions from all authors.

Competing interests

The authors declare no competing interests.

Additional information

Supplementary information is available for this paper at https://doi.org/10.1038/s41567-019-0670-x.

Correspondence and requests for materials should be addressed to S.R. or N.P.B.

Methods

Single crystals of UTe_2 were synthesized by the chemical vapour transport method using iodine as the transport agent. Crystal orientation was determined by Laue X-ray diffraction performed with a Photonic Science X-ray measurement system. Magnetoresistance measurements were performed at the National High Magnetic Field Laboratory (NHMFL), Tallahassee, using the 35 T d.c. magnet, and at NHMFL, Los Alamos, using the 65 T short-pulse magnet. PDO and magnetization measurements were performed at NHMFL, Los Alamos, using the 65 T short-pulse magnet.

To perfectly align the magnetic field along the b axis in the d.c. magnet, a single crystal of Ute_2 was fixed to a home-made sample mount on top of an Attocube ANR31 piezo-actuated rotation platform (Fig. 1b). Thin copper wires were fixed between the probe and rotation platform, in order to measure the sample and two orthogonal Toshiba THS118 Hall sensors. All three measurements were performed using a conventional four-terminal transport set-up with Lake Shore Cryotronics 372 a.c. resistance bridges. Adjustments to θ were made using a low-friction apparatus[28] to find the centre of the range, where the sample resistance was zero at $H = 25.5$ T. With a lower field of 0.5 T, small changes were then made to the ϕ orientation while monitoring the Hall sensors. With the field aligned near the b axis, the magnetic field was swept to 34.5 T.

The contactless conductivity was measured using the PDO circuit described in refs. [29,30] that has been used to study field-stabilized superconducting phases[31]. A coil comprising 6–8 turns of 46-gauge high-conductivity copper wire was wound about the single-crystal sample; the number of turns employed depends on the cross-sectional area of the sample, with a larger number of turns needed for smaller samples. The coil formed part of a PDO circuit resonating at 22–29 MHz. A change in the sample skin depth[29] or differential susceptibility[30] causes a change in the inductance of the coil, which in turn alters the resonant frequency of the circuit. The signal from the PDO circuit was mixed down to about 2 MHz using a double-heterodyne system[29,30]. Data were recorded at 20 million samples per second, well above the Nyquist limit. Two samples in individual coils coupled to independent PDOs were measured simultaneously using a single-axis, worm-driven, cryogenic goniometer to adjust their orientation in the field.

The pulsed field magnetization experiments used a 1.5-mm-bore, 1.5-mm-long, 1,500-turn compensated-coil susceptometer constructed from 50-gauge high-purity copper wire[32]. When a sample is within the coil, the signal is proportional to dM/dt, where M is magnetization and t is time. Numerical integration was used to evaluate M. The sample was mounted within an ampoule of 1.3 mm diameter that could be moved in and out of the coil. Accurate values of M were obtained by subtracting empty coil data from that measured under identical conditions with the sample present. These results were calibrated against results from the Quantum Design's magnetic property measurement system.

Data availability

The data represented in Figs. 1–4 are available as source data in Supplementary Data 1–4. All other data that support the plots within this paper and other findings of this study are available from the corresponding authors on reasonable request.

References

28. Palm, E. C. & Murphy, T. P. Very low friction rotator for use at low temperatures and high magnetic fields. *Rev. Sci. Instrum.* **70**, 237–239 (1999).
29. Altarawneh, M. M., Mielke, C. H. & Brooks, J. S. Proximity detector circuits: an alternative to tunnel diode oscillators for contactless measurements in pulsed magnetic field environments. *Rev. Sci. Instrum.* **80**, 066104 (2009).
30. Ghannadzadeh, S. et al. Measurement of magnetic susceptibility in pulsed magnetic fields using a proximity detector oscillator. *Rev. Sci. Instrum.* **82**, 113902 (2011).
31. Singleton, J. et al. Observation of the Fulde–Ferrell–Larkin–Ovchinnikov state in the quasi-two-dimensional organic superconductor κ–(BEDT–TTF)$_2$Cu(NCS)$_2$. *J. Phys. Condens. Matter* **12**, L641 (2000).
32. Goddard, P. A. et al. Experimentally determining the exchange parameters of quasi-two-dimensional Heisenberg magnets. *New J. Phys.* **10**, 083025 (2008).